ISSN (Print) 1226-1750
ISSN (Online) 2233-6656
Journal of Magnetics 31(3), 438-448 (2026) https://doi.org/10.4283/JMAG.2026.31.3.438

Multibeam Antenna Array Design for Millimeter Wave Vehicle-to-Everything (5G-V2X)

Moubarek Traii[1,2], Mohamed Fawar[1], Zied Harouni[1,3], Ahmed Laiche[1]*, Ridha Ghayoula[4], Said Ghnimi[1], and Ali Gharsallah[1]

[1]*Laboratory of Microwave Electronics, Faculty of Sciences of Tunis, University of Tunis El Manar, Tunis 2092, Tunisia*
[2]*National Engineering School of Bizerte, Carthage University, 1054 Amilcar, Tunisia*
[3]*Higher School of Communication, Carthage University, 1054 Amilcar, Tunisia*
[4]*Department of Computer Science and Software Engineering, Laval University, QC G1V4G5, Canada*

(Received 16 July 2026, Received in final form 5 September 2026, Accepted 10 September 2026)

This paper presents a reconfigurable antenna array operating at 28 GHz for fifth-generation (5G) Vehicle-to-Everything (V2X) communications. The proposed design employs a hybrid multilayer architecture comprising four compact Yagi–Uda antenna elements integrated with PIN diode-controlled parasitic structures to enable dynamic beam reconfiguration. By selectively controlling the PIN diodes, the surface current and associated magnetic field distributions are reconfigured, producing three distinct radiation modes: end-fire toward the negative z-direction, central end-fire, and end-fire toward the positive z-direction. This controlled redistribution of the magnetic field enhances electromagnetic coupling between the driven and parasitic elements, resulting in efficient beam switching in the azimuth and elevation planes. Consequently, the array provides wide/cumulative azimuthal coverage through switching among multiple radiation states, with a vertical steering range of ±30° while maintaining a gain variation below 1 dB. Simulation results demonstrate a peak realized gain of 14.47 dBi, port isolation exceeding 20 dB, and a wide impedance bandwidth ($|S_{11}| < -10$ dB) extending from 23.28 to 29.31 GHz. These results confirm that the proposed reconfigurable array achieves high-gain, wideband, and electronically reconfigurable switched-beam operation, making it a promising candidate for reliable millimeter-wave 5G V2X communications and next-generation intelligent transportation systems.

Keywords : reconfigurable antennas, 5G network, beamforming antenna array, multilayer design, electro-magnetic field

1. Introduction

In recent years, the telecommunications sector has undergone significant transformation, driven by major advances in wireless communication systems and the emergence of fifth-generation (5G) technologies. A key characteristic of 5G lies in its ability to provide seamless connectivity across multiple wireless platforms, allowing users to switch effort lessly between different access technologies [1-23]. This generation of communication systems particularly benefits devices supporting Voice over IP (VoIP), offering data rates suitable for high-speed transmission and high-quality communications, thereby addressing users' increasing demand for advanced digital services.

To achieve these performance levels, 5G systems exploit new spectral resources, especially the millimeter-wave (mmWave) frequency band, which constitutes a specific portion of the electromagnetic spectrum. This band supports ultra-high-speed communications for both mobile terminals and backhaul links between small cells [2]. Still relatively underutilized, it offers considerable potential, particularly within the 28 GHz, 38 GHz, 71–76 GHz, and 81–86 GHz ranges, which have been identified as highly promising. Millimeter-wave frequencies enable the design of compact, high-efficiency RF structures suitable for both base-station equipment and vehicular applications [3].

Autonomous vehicles are increasingly shaping the automotive sector owing to their capacity to sense and interpret their environment, thereby enhancing both road safety and passenger comfort [4]. However, their performance

©The Korean Magnetics Society. All rights reserved.
*Corresponding author: Tel: +21658828350
E-mail: ahmed.laiche@fst.utm.tn

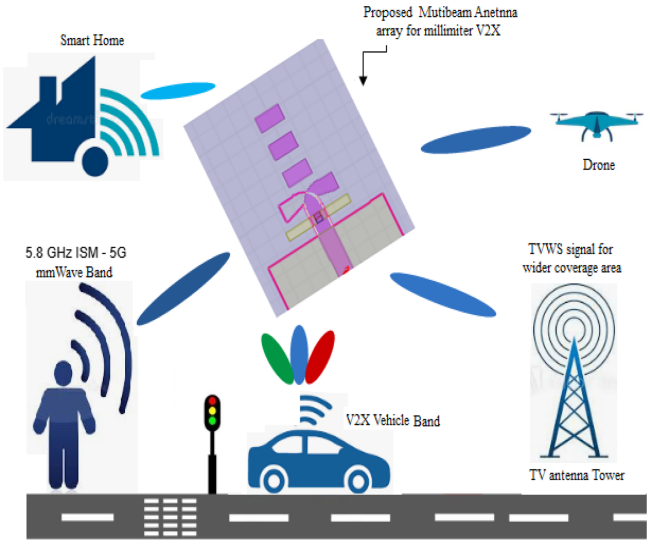


Fig. 1. (Color online) Diagram of mmWaves 5G V2X communications in the Advanced transportation ecosystem.

remains limited without direct, reliable communication among vehicles sharing the same road infrastructure [5]. To overcome this limitation, dependable and high-capacity connectivity is required to enable the real time exchange of critical information between vehicles and surrounding infrastructure, as illustrated in Fig. 1.

In this context, the integration of antennas represents a major challenge due to the physical constraints imposed by vehicle structures. Antennas must be simple to design and compatible with the mechanical architecture of vehicles, without affecting aerodynamics or energy efficiency, while ensuring optimal signal performance under mobility, obstacles, and interference conditions [6]. For these reasons, V2X technology has been developed primarily to enhance road safety by reducing the risk of accidents. In addition, it enables more efficient data exchange between vehicles and their surrounding environment, paving the way for innovative solutions aimed at decreasing traffic congestion and contributing to the development of smart cities and next-generation transportation systems [7].

In parallel with these technological advances, antennas dedicated to automotive platforms must also address several technical challenges, such as main beam shaping and side-lobe suppression, which are decisive for system performance. The efficiency of antenna arrays depends largely on their ability to focus radiated energy in a desired direction while reducing interference and preventing energy propagation toward undesired directions [8]. To meet these requirements, several optimization techniques have been proposed. In this work, the Taguchi method is selected due to its simplicity and robustness, offering an efficient statistical approach for parameter optimization using a reduced number of iterations [9].

Despite recent progress, limited studies have systematically investigated the impact of structural deformation on key performance metrics such as isolation, diversity gain, and envelope correlation coefficient in multibeam antenna arrays. To address this gap, this paper presents the design and comprehensive evaluation of a multibeam antenna array operating in the millimeter-wave band for intelligent automotive applications. The proposed system realizes a switched-beam antenna capable of focusing on a desired user while mitigating multipath effects, noise, and interference, thereby enhancing overall system capacity. Electromagnetic performance is analyzed using the 3D full-wave simulator HFSS under various bending conditions and realistic loading scenarios, including body interaction. The results demonstrate the robustness of the proposed design and its ability to maintain stable performance, supporting the development of reliable, high-performance wearable and automotive antenna systems for practical applications.

The main novelty of this work is the development of a compact multilayer Yagi–Uda-inspired four-element antenna array with PIN-diode-controlled parasitic structures for reconfigurable 28-GHz 5G-V2X communications. Unlike conventional fixed-beam antenna arrays, the proposed configuration enables electronic switching of the radiation direction through controlled redistribution of the surface current and magnetic-field distributions. The proposed architecture combines reconfigurable end-fire beam steering in the ±z directions, a central/symmetric radiation mode, wide impedance bandwidth, high array gain, and compact multilayer implementation within a single antenna structure. In particular, the optimized three-director configuration provides a compromise between directivity, gain, front-to-back ratio, and bandwidth, while the four-element array increases the peak realized gain to 14.47 dBi. The resulting simulated impedance bandwidth extends from approximately 23.28 to 29.31 GHz, with port isolation exceeding 20 dB. These characteristics distinguish the proposed design from conventional fixed-beam and less spatially flexible reconfigurable antennas and make it suitable for dynamic V2X environments requiring adaptive spatial coverage and reliable millimeter-wave communication.

The organization of this paper is as follows. Section 1 introduces the fundamental concepts of millimeter-wave antenna arrays and reviews key 5G technologies, including beamforming, massive MIMO, and full-duplex communication. Section 2 presents the design and optimization of a multilayer Yagi–Uda antenna for V2X applications, highlighting the integration of PIN diodes for electro-

magnetic reconfiguration. Section 3 focuses on the development and analysis of a reconfigurable antenna array using PIN diodes to enhance gain and coverage. Finally, Section 4 concludes the paper, summarizes the main findings, and outlines future research directions.

2. Antenna Design and Optimization

The new generation of reconfigurable antennas plays a key role in modern wireless communication systems due to their ability to dynamically modify their electromagnetic characteristics [10]. They are widely employed in several applications, including satellite communications; direct broadcast systems (DBS), automotive radar, and V2X platforms, where adaptive spatial coverage and enhanced reliability are required, especially in dynamic and constrained environments. According to the limitations reported in [11], including reduced communication coverage in specific directions, relatively lower gain in inclined modes (end-fire ±z), and elevated side-lobe levels for certain configurations, there is a clear need for an improved antenna design. In particular, the gain may fall below 8 dBi in some orientations, potentially compromising link robustness in challenging urban and mobile environments, such as tunnels, curved road sections, and obstacle-dense areas. Furthermore, the presence of pronounced side lobes can increase undesired radiation and interference [12], thereby reducing beam directivity and potentially degrading the overall communication quality. These limitations motivate the development of an antenna configuration capable of providing more uniform gain, improved directional control, and reduced side-lobe levels across the required radiation modes.

2.1. RF Switch Configurations and Modeling

Antenna characteristics may be reconfigured by integrating electronic switching components such as PIN diodes (for millimeter-wave frequencies) [13], varactor diodes, MES FET transistors (Metal–Semiconductor Field Effect Transistor), or MEMS (Micro–Electro–Mechanical System) devices acting as switches or variable capacitors. These components enable selectable radiation beam configurations.

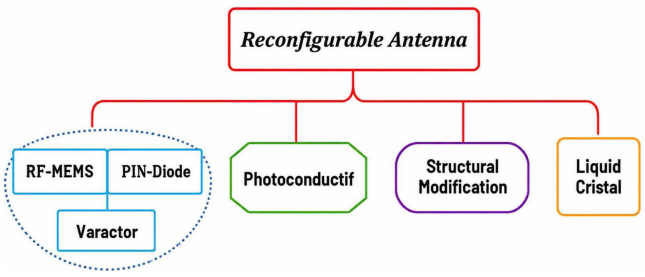


Fig. 2. (Color online) Different configuration techniques for reconfigurable antennas.

In this work, a PIN diode is selected to control the radiation pattern, the beamwidth, and the beam steering direction. Owing to its very short switching time, the PIN diode is among the most commonly used RF components.

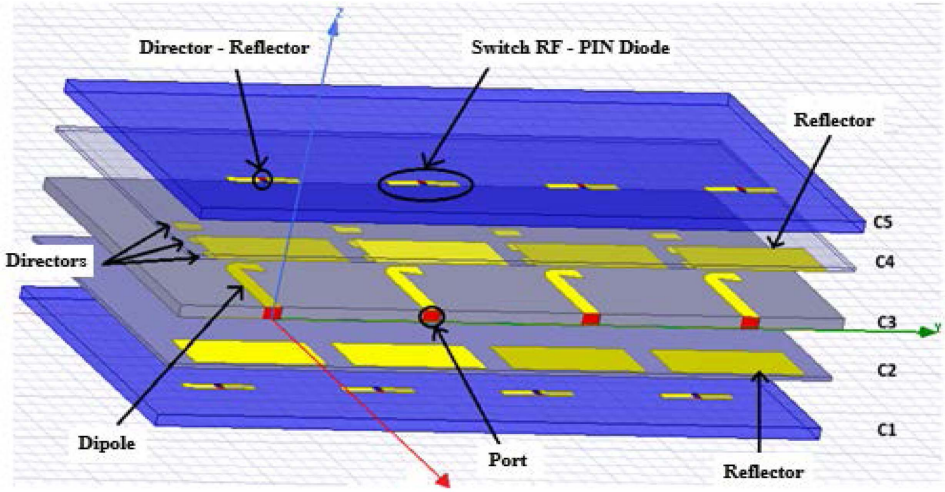
- *PIN diodes states in operating modes:* The PIN diode is one of the most common radio frequency components because its switching time is relatively very short. PIN diodes are widely used in radio frequency and microwave systems for various functions such as attenuation [14], switching (e.g., antenna switching between transmitter and receiver), controllable phase shifting, inductance switching to cover a wide frequency band in multiband receivers, and amplitude modulation of RF signals. Next step is to design a PIN diode RF switch using ADS software by applying forward bias to turn the diode on (End fire +Z) and reverse bias to turn it off (End fire -Z).

The switch design is guided by key performance parameters, which are presented together with the circuit schematics of both simple and compound switch configurations. The proposed design is based on a symmetrical linear two-port network topology, providing a structured framework for analyzing and optimizing the switch performance. The impedance characteristics (Zo) of the input power source, the switch structure, the load impedance, and any transmission lines connecting these components are all 50 Ohms.

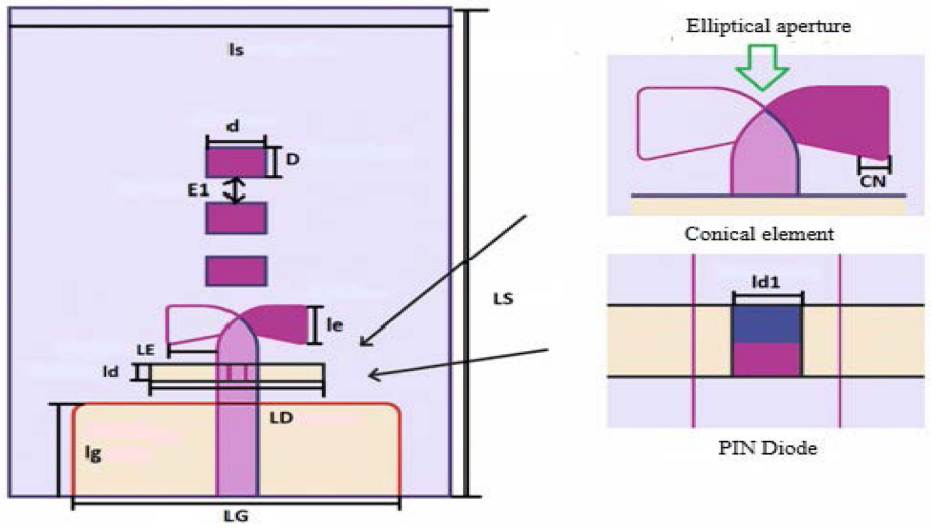
- *Series SPST Switch:* A PIN diode SPST can be used in broadband configurations. Both the power dissipation and the insertion loss depend on the forward-biased series resistance (Rs) of PIN diode [15]. The maximum isolation achievable depends on the capacitance of the diode (Ct). The ISO and IL equations, as well as the performance characteristics, are given below.

2.2. Proposed Single Element using PIN-Diode RF Switch

In this contribution, a compact dipole antenna with wide spatial coverage and a reconfigurable radiation pattern is proposed for V2X applications operating in the 28-32 GHz band. The architecture is based on an enhanced multilayer planar Yagi–Uda antenna topology. The developed structure provides two distinct operating configurations derived from geometric modifications of both the driven and director elements. The proposed design features conical driven elements with an elliptical aperture and identical conventional directors replacing standard uniform rectangular strips. These modifications



(a)



(b)

Fig. 3. (Color online) (a) Detailed view of the substructure comprising four elements, (b) ULB antenna geometry.

are mainly applied to the third and fourth PCB layers, which accommodate the dipole-based radiating structure, including the driven element, director, and reflector, as illustrated in Fig. 2.

The main radiating element features a symmetrical conical shape with an elliptical aperture. The integration of three identical reflectors enhances the antenna's bandwidth, improves the front-to-back ratio (F/B), and significantly increases the achievable gain compared to rectangular dipole structures presented in [16].

The proposed antenna is implemented on a five-layer board composed of three substrate layers, designated C1, C3 and C5, using Rogers RO4003C material. These layers have a relative permittivity of (ε_r = 3.55), a loss tangent of (tan δ = 0.0027), and a thickness of 0.6 mm each. The two intermediate substrate layers, designated C2 and C4, are fabricated using Rogers RO4350B, with a relative permittivity of (ε_r = 3.66), a loss tangent of (tan δ = 0.0037), and a thickness of 0.2 mm each. The upper and lower layers accommodate the director and reflector structures, respectively, while the integrated PIN diodes operate as RF switches to control the different radiation states of the antenna array. The complete multilayer configuration is modeled using the full-wave CST electromagnetic solver at 28 GHz. The conductor material and thickness, together with the simulation boundary conditions, are specified to ensure accurate and reproducible electromagnetic analysis.

Table 1. Antenna dimensions expressed in millimeters, based on the wavelength λ.

Symbol	Definition	Dimension Size in (mm)
LS	Total substrate length	12
ls	Total substrate width [1]	7.5
LG	Ground plane length	7.5
Lg	Ground plane width	2.5
LE	Radiating element length	1.2
Ld	Diode band width	0.5
LD	Diode band length	0.5
Le	Radiating element width	1
E1	Distance between directors	0.6
CN	Dipole length	0.5
Id1	PIN diode width	0.2

Multilayer antenna architecture is designed to achieve high directivity while maintaining reduced physical dimensions, ensuring extensive coverage in both elevation and azimuth planes, and meeting stringent constraints associated with vehicular platforms [17].

2.2.1. Influence of Director Configuration on the Antenna Characteristics

To evaluate the influence of the directors on the antenna's performance, three structural configurations were investigated. Each configuration incorporates a different number of directors (2, 3, and 4), with the objective of analyzing their effects on gain, bandwidth, and radiation directivity characteristics.

In the two-director antenna configuration (Fig. 4a), a slight improvement in gain was achieved, but at the cost

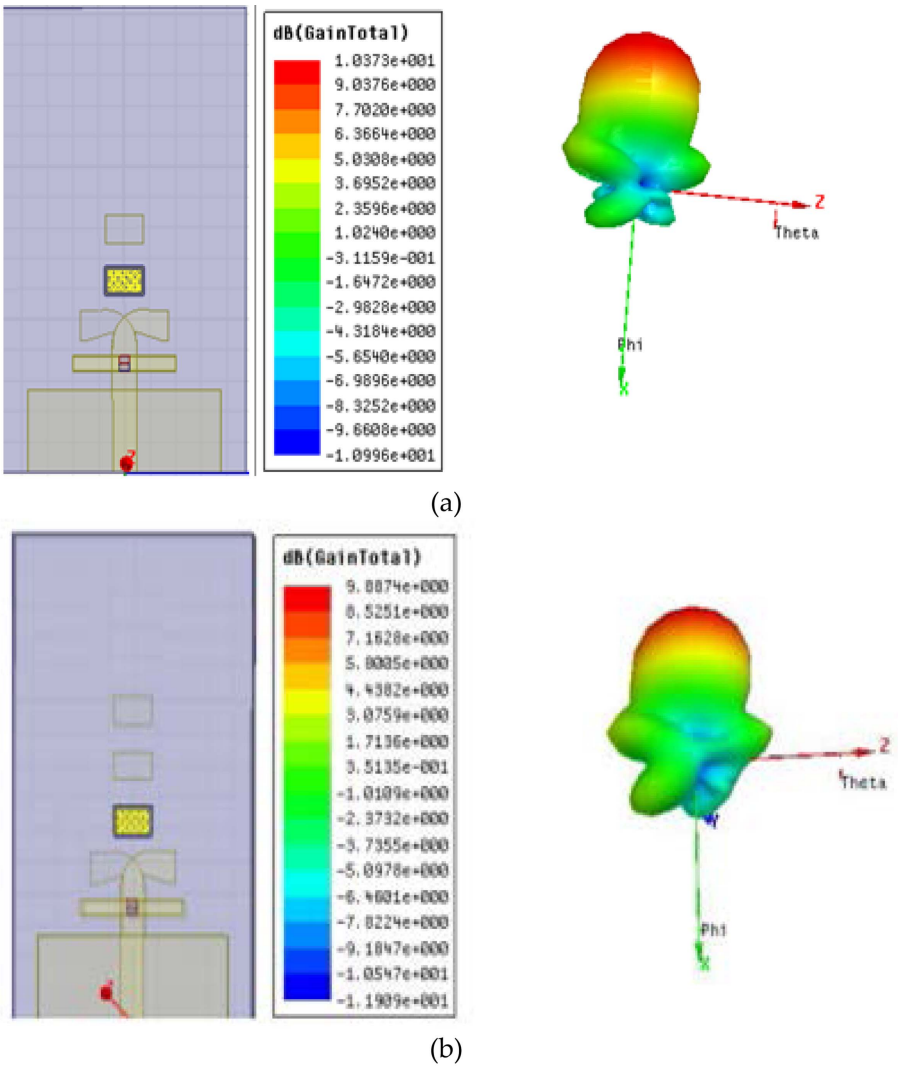
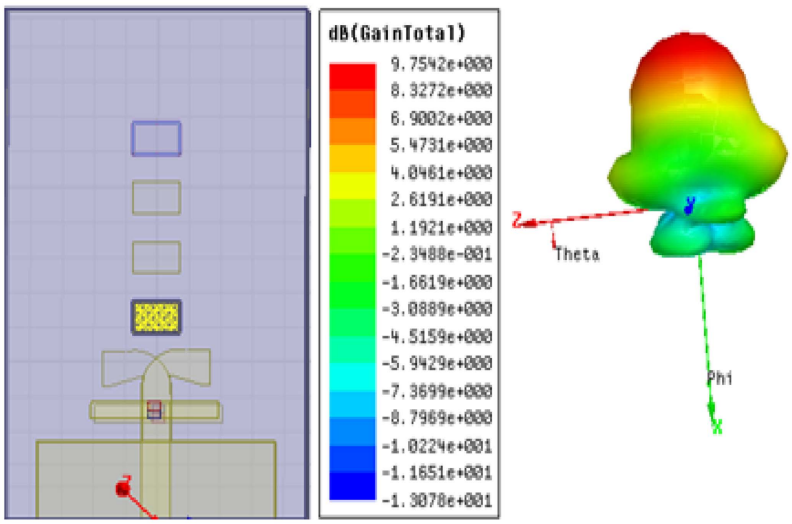


Fig. 4. (Color online) Effect of the number of directors on antenna performance: (a) two directors, (b) three directors, and (c) four directors.



(c)

Fig. 4. Continued.

of a reduction in bandwidth of approximately 0.7 GHz.

The four-director antenna (Fig. 4c) presents a gain that decreases with an increase in the number of directors, which can be attributed to an imbalance in the distribution of the radiated field. On the other hand, the front-to-back ratio tends to improve with a larger number of directors, indicating a more significant concentration of radiation toward the front.

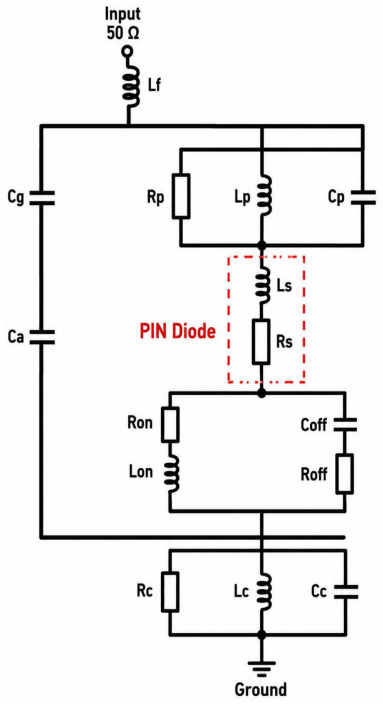


Fig. 5. (Color online) Equivalent circuit model of the proposed antenna in the ON state.

However, the configuration incorporating three directors (Fig. 4b), as adopted in the proposed structure, proved to be the best compromise in terms of overall electromagnetic performance. Not only does it optimize directivity and improve the front-to-back (F/B) ratio, but it also preserves a wide bandwidth.

2.2.2. Equivalent circuit model of Single Element

Based on the geometry in your Fig. 4, this is a reconfigurable multilayer antenna composed of a microstrip feed line, a rectangular ground plane, a radiating patch with an elliptical aperture, a conical metallic element, a PIN diode connecting two metallic sections and two dielectric layers (multilayer substrate).

The equivalent circuit can therefore be represented by several coupled resonators in Fig. 5.

Table 2 describes the components of the proposed

Table 2. lists the equivalent circuit components along with their corresponding physical meanings and functions in the proposed multilayer antenna.

Component	Physical meaning
Lf	Feed-line inductance
Cg	Feed-to-ground capacitance
Rp	Radiation and conductor losses
Lp	Current path on the patch
Cp	Patch-to-ground capacitance
Ca	Coupling capacitance through the elliptical aperture
Rc-Lc-Cc	Conical resonator
Rs-Ls	PIN diode Switching element (on state)
Ground	Ground plane

equivalent circuit and their corresponding physical interpretations.

The proposed equivalent circuit provides a physical representation of the electromagnetic behavior of the multilayer reconfigurable antenna. The inductive elements model the magnetic energy associated with surface currents, whereas the capacitive elements represent the electric coupling between the metallic layers and the ground plane. The PIN diode acts as a reconfigurable impedance, modifying the current path and magnetic-field distribution. In the ON state, it extends the effective electrical length, shifting the resonance to lower frequencies, while in the OFF state, it interrupts the current flow, reducing electromagnetic coupling and exciting different resonant modes. The agreement between the simulated magnetic-field distributions and the equivalent circuit validates the proposed model, demonstrating that beam reconfiguration and frequency tuning are achieved through controlled current redistribution. This behavior significantly enhances the electrical and radiation performance of the proposed antenna.

To further clarify the physical mechanism responsible for beam reconfiguration, the simulated surface-current distributions are investigated for the different PIN-diode switching states at 28 GHz. As illustrated in Fig. 10, changing the diode state modifies the current path on the driven and parasitic elements and consequently changes the electromagnetic coupling between adjacent elements. When the PIN diode is in the ON state, the conductive connection extends the effective current path, whereas in the OFF state, the current path is interrupted. These changes produce different amplitude and phase distributions of the surface currents along the Yagi–Uda elements. As a result, the radiated fields combine constructively in different directions, leading to the observed switching between the +z and −z end-fire radiation modes. The surface-current distributions therefore provide physical evidence that the beam reconfiguration is achieved through controlled redistribution of the electromagnetic current and magnetic-field distributions rather than by changing the physical orientation of the antenna.

2.2.3. Results and Discussion of Single Element

It is important to emphasize that the antenna operates in end-fire mode, meaning that the main lobe is oriented along the axis of the antenna, radiating predominantly in the forward direction.

Figure 6 presents the simulated reflection coefficient (S_{11}). The multilayer single element antenna was designed and simulated using HFSS, where optimal radiation characteristics were obtained through the fine adjustment

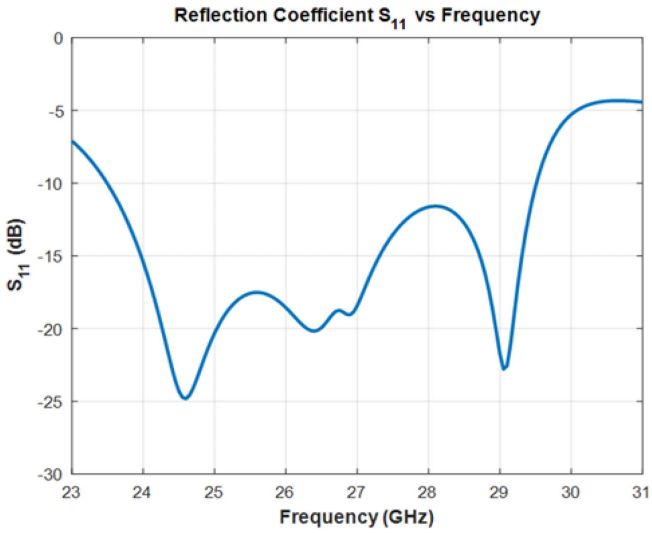


Fig. 6. (Color online) Reflection coefficient responses of the proposed multilayer single antenna.

of key structural parameters.

This Fig. 6 shows that the −10 dB bandwidth extends from 23.37 GHz to 29.31 GHz, covering a relatively wide frequency range with three resonance modes. This behavior demonstrates good impedance matching over the operating band, and consequently acceptable radiation efficiency. It can also be observed that the use of a multilayer structure contributes to a significant bandwidth enhancement and improved overall performance of the ULB configuration. The proposed design maintains a wide operating band while offering substantial improvements in other key performance parameters. This multiband operation remains suitable for millimeter-wave applications and provides enhanced flexibility and reconfig-

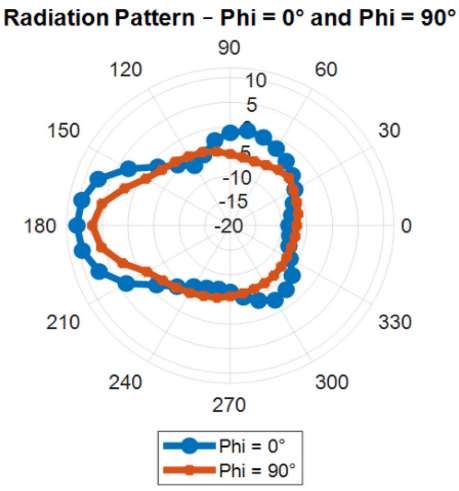


Fig. 7. (Color online) Simulated E-plane and H-plane at 28 GHz for the multilayer single element antenna.

urability compared to the basic structure.

The radiation patterns of the proposed antenna were simulated in the two principal planes, namely the E-plane (X–Z plane) and H-plane (Y–Z plane), at 28 GHz, as illustrated in Fig. 7. The results demonstrate that the proposed antenna exhibits highly directional radiation characteristics in both planes, with the radiated energy concentrated toward specific directions. This directional behavior enables effective beam steering and enhanced spatial coverage, making the proposed design suitable for high-frequency V2X communication applications.

It can be seen that in the vertical plane, the antenna has a smaller angular aperture compared to the horizontal plane. This limited vertical directivity is a characteristic of the initial passive structure. However, this aperture can be increased by activating PIN diodes, allowing switching between the two end-fire directions +z and –z, which enhances radiation flexibility in the rise plane.

2.3. Design of a Reconfigurable 4-Element Antenna

To provide extended spatial coverage and support high data traffic while ensuring seamless integration into existing vehicular communication infrastructures, the design of a four-element reconfigurable antenna array is proposed. This configuration represents a significant advancement in the field of 5G millimeter-wave systems. Fig. 8 illustrates the geometry of the four-element reconfigurable array, where the diode switching states are configured as ON–OFF / ON–OFF.

The four-element antenna array was designed to achieve sufficient overall gain and effective beam-steering performance. However, the number of elements is not limited to four and can be increased to attain higher gain. In this study, the beam-steering analysis was performed using a four-element configuration (Fig. 8).

It should be noted that the proposed architecture provides switched-beam operation rather than continuous electronic beam steering. The overall azimuthally coverage is obtained cumulatively by switching among the available PIN-diode configurations, with each configuration producing a specific radiation pattern.

The main objective of this design is to provide a compact antenna module capable of optimizing system performance while ensuring wide spatial coverage, reduced complexity, controlled costs, and straight forward integration into existing vehicular communication infrastructures.

2.3.1. Simulated Results and Discussion of Antenna Array

Figure 9 illustrates the reflection coefficient responses S_{11}, S_{22}, S_{33}, and S_{44} of the antenna array in end-fire mode –z, where diodes D11, D12, D13, and D14 are activated and the upper layer diodes D21, D22, D23, and D24 are deactivated. A clear double resonance can be observed at 23.70 GHz and 26.75 GHz, with a minimum reaching –17.64 dB and –22.61 dB, respectively.

S_{ii} is the reflection coefficient of antenna i, which is the part of the signal that is reflected back to port i, where:

S_{11}: antenna reflection coefficient 1,
S_{22}: antenna reflection coefficient 2,
S_{33}: antenna reflection coefficient 3,
S_{44}: antenna reflection coefficient 4

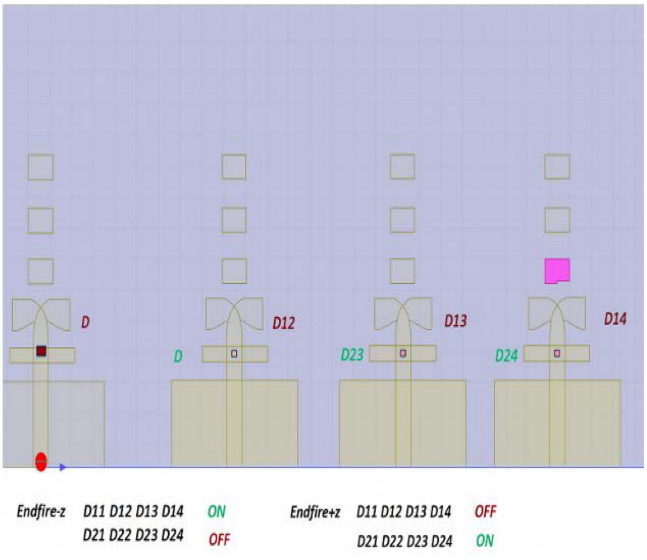


Fig. 8. (Color online) Antenna array geometry with ON-OFF/ ON-OFF diode state.

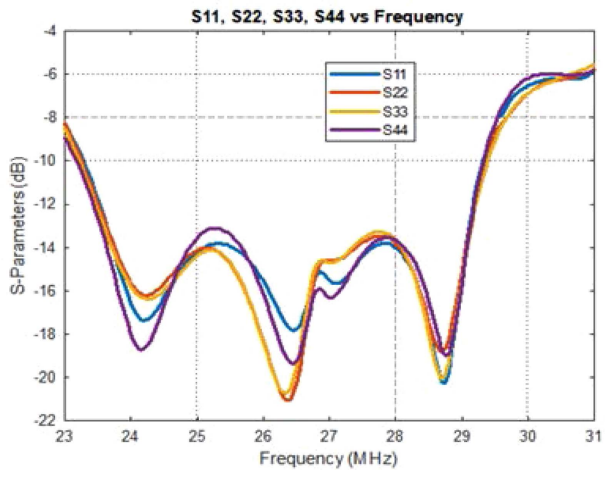


Fig. 9. (Color online) Reflection coefficient responses S_{11}, S_{22}, S_{33}, and S_{44} of the four-element antenna array in end-fire −z mode.

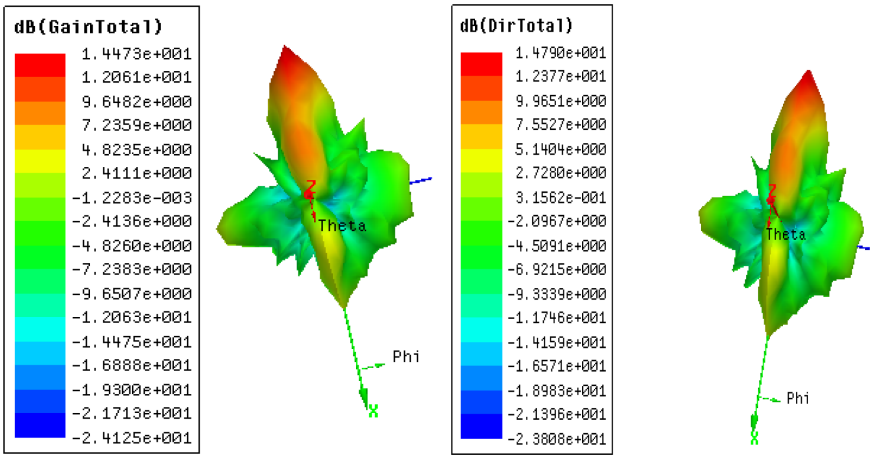


Fig. 10. (Color online) Gain and directivity of an antenna network in endfire mode.

The analysis of the S parameters of the 4-element network is illustrated in the following figure.

The Fig. 9 above shows a good adaptation (less than –10 dB) over a wide bandwidth extending from 22.6 GHz to 29.13 GHz, indicating efficient operation in this configuration mode.

The 3D radiation pattern study of the 4-element array antenna is performed on two successive states of diode configuration (Fig. 10).

ON-ON state:

As shown in Fig. 10, the antenna gain increases from 10.25 dBi for a single radiating element to 14.47 dBi for the four-element array. This improvement demonstrates the benefit of increasing the number of radiating elements in enhancing the overall gain and directivity of the proposed antenna. This behavior is consistent with the fundamental operating principle of antenna arrays, in which the coherent combination of the electromagnetic fields radiated by the individual elements results in a more focused radiation pattern and increased array directivity.

ON-OFF/ON-OFF state:

The Fig. 11 shows a main lobe directed along the z-axis in both directions (±z), clearly illustrating the reconfigurable endfire operation. The maximum gain reaches 13.39 dBi in the +z direction and 14.17 dBi in the –z direction, which represents a significant improvement over the reference structure.

Beam Alignment: Beam inclination refers to the angular displacement of an antenna's main radiation direction relative to a reference direction [18], usually the axis perpendicular to the antenna (often 0° or 90° depending on the plane studied).

In the context of x-z plane, the angle of inclination corresponds to the angle at which maximum gain is observed, thus indicating the preferred direction of radiation.

Figure 12 illustrates the normalized realized gain as a function of angle together with the corresponding two-dimensional radiation pattern for the end-fire operating

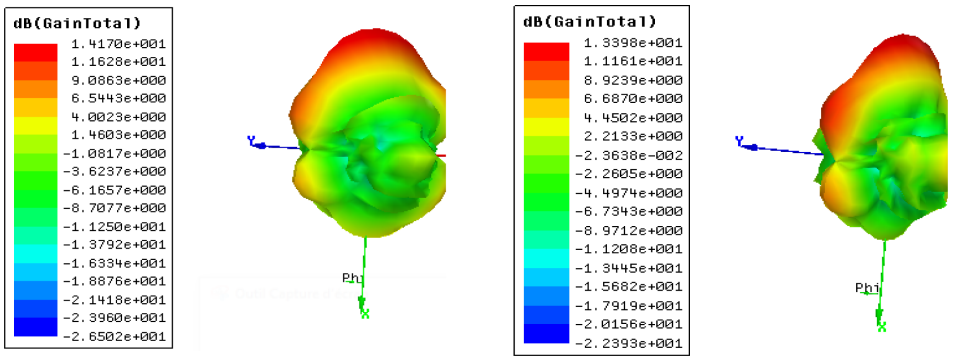


Fig. 11. (Color online) Antenna gain in [dB] as a function of frequency in endfire-z/+z modes.

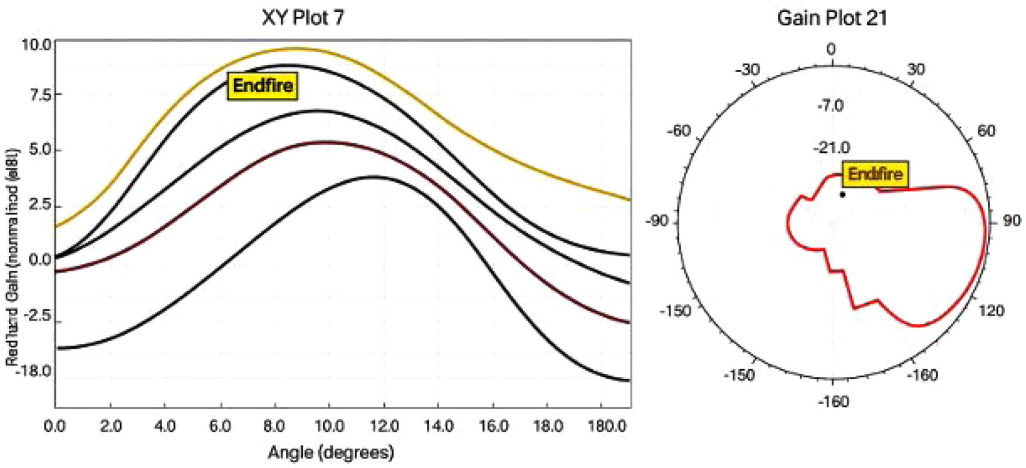


Fig. 12. (Color online) Antenna gain in [dB] as a function of frequency in endfire-z/+z modes.

Table 3. Comparison of the proposed antenna with recently reported designs.

Reference	Frequency (GHz)	Bandwidth (GHz)	Peak gain (dBi)	Efficiency
Ref. [11]	27	25.24-28.76	7.5	0.45
Ref. [16]	27.4	24.8-28.1	8.9	0.47
Proposed Work	28	22.6-29.13	14.47	0.78

mode. The gain curves exhibit a pronounced maximum in the end-fire direction, indicating that the electromagnetic energy is efficiently guided and radiated along the antenna axis. As the observation angle deviates from the main beam, the gain gradually decreases, demonstrating effective suppression of radiation in undesired directions. The polar radiation pattern confirms a highly directive end-fire beam with a well-defined main lobe and relatively low back radiation, which is characteristic of Yagi–Uda antenna arrays.

The observed radiation characteristics imply that the magnetic field is predominantly confined near the active and parasitic elements before being transformed into a directive far-field radiation pattern. Reconfiguration of the PIN diode states alters the near-field magnetic coupling between adjacent elements, thereby switching the direction of maximum radiation without significantly affecting the peak gain. This controlled redistribution of the magnetic field enables efficient beam switching while preserving high directivity and stable radiation performance.

To further assess the performance of the proposed antenna, a comparison with recently reported millimeter-wave and reconfigurable antenna designs is presented in Table X. The comparison considers the operating frequency, impedance bandwidth, peak gain, radiation efficiency, number of elements, overall dimensions, port isolation, and beam-reconfiguration capability. As shown in Table X, the proposed four-element array provides a favorable combination of wide bandwidth, high gain, good isolation, and electronically reconfigurable end-fire radiation at 28 GHz. These characteristics make the proposed configuration particularly attractive for compact and dynamically reconfigurable V2X communication systems.

It can be observed that the proposed antenna achieves a competitive overall performance, particularly in terms of peak gain, bandwidth, and beam reconfigurability, while maintaining a compact four-element architecture.

3. Conclusions

This work has developed and evaluated a reconfigurable multibeam antenna array operating at 28 GHz, targeting 5G Vehicle-to-Everything (V2X) communication systems. A multilayer Yagi–Uda-inspired configuration with PIN diode integration was introduced to realize electronically reconfigurable switched-beam operation and radiation pattern reconfiguration. The proposed design enables switching among multiple end-fire radiation states (−z, +z, and a symmetric mode), thereby improving spatial coverage in both azimuth and elevation directions, which is essential for dynamic vehicular scenarios.

The single-element study demonstrated stable radiation behavior with wide impedance bandwidth, while the four-

element array configuration achieved a maximum gain of 14.47 dBi, along with good port isolation and effective beam switching control. The use of PIN diode states provided flexible radiation reconfiguration, enhancing the antenna's suitability for rapidly changing propagation environments in V2X systems.

Overall, the results confirm that the proposed antenna system satisfies key 5G-V2X requirements, including high gain, reconfigurability, beam agility, and interference resilience, making it a strong candidate for next-generation intelligent transportation communication networks.

Acknowledgements

The authors would like to express their sincere gratitude to the Laboratory of Microwave Electronics at the Faculty of Sciences of Tunis, University of Tunis El Manar, for providing the research facilities and technical support that made this work possible.

References

[1] Y. O. Imam-Fulani, N. Faruk, O. A. Sowande, A. Abdulkarim, E. Alozie, A. D. Usman, K. S. Adewole, A. A. Oloyede, H. Chiroma, S. Garba, A. L. Imoize, B. A. Baba, A. Musa, Y. A. Adediran, and L. S. Taura, Sustainability **15**, 5173 (2023).

[2] O. O. Erunkulu, A. M. Zungeru, C. K. Lebekwe, M. Mosalaosi, and J. M. Chuma, IEEE Access **9**, 97251 (2021).

[3] Z. Wang, S. Liu, and Y. Dong, IEEE Transactions on Antennas and Propagation **70**, 7199 (2022).

[4] M. M. Rahman and J. C. Thill, Sustainability **15**, 11541 (2023).

[5] S. Refas, D. Acheli, S.Yahia, Y. Meraihi, A. R. Cherif, N. V. Van, and T. D. Ho, IEEE Access **11**, 129436 (2023).

[6] Z. Shahbazid and S. Nowaczyk, Smart Cities **6**, 2574 (2023).

[7] S. Chavhan, R. Doswada, D. Gupta, S. Gunjal, and J. J. P. C. Rodrigues, IEEE Transactions on Consumer Electronics Society **71**, 1926 (2025).

[8] I. S. Dmitriev, O. N. Zavalishina, and M. P. Slichenko, J. Radioengineering **88**, 16 (2024).

[9] W. C. Weng, F. Yang, and A. Z. Elsherbeni, IEEE Transactions on Antennas and Propagation **55,** 723 (2007).

[10] K. Ramahatla, M. Mosalaosi, A. Yahya, and B. Basutli, IEEE Access **10**, 40910 (2022).

[11] W. Kim, Sensors **19**, 2057(2019).

[12] C. Vijay, L. Bassa, V. Gunda, S. Devakivada, and G. V. S. M. Vignesh, IEEE Wireless Antenna and Microwave Symposium, 1 (2024).

[13] N. O. Parchin, H. J. Basherlou, Y. I. A. Al-Yasir, A. M. Abdulkhaleq, and R. A. Abd-Alhameed, Electronics **9**, 336 (2020).

[14] B. Boyapati and J. Kumar, Advances in Technology Innovation **8**, 210 (2023).

[15] P. Sun, L. Peng, P. Upadhyaya, and D.-H. Jeong, Microwave and Optical Technology Letters **53**, 1430 (2011).

[16] S. Islam, H. Kim, T. D. Nguyen, S. Kim, and H. Yoo, IEEE Access **13**, 8740 (2025).

[17] S. Seo, W. Kim, H. Park, Y. Seo, D. Park, H. Kim, K. Lee, H. Lee, and S. Kahng, Sensors **24**, 6831 (2024).

[18] S. Y. Liu, C. F. Zhou, J. Liu, J. H. Fu, Q. Wu, and X. M. Ding, IEEE Open Journal of Antennas and Propagation, **3**, 1218 (2022).

[19] P. A. Mezhevov, K. O. Korovin, and A. N. Likontsev, Journal of the Russian Universities. Radioelectronics. **26**, 58 (2023).

[20] K. Shao, H. Fu, and B. Wang, J. Electronics **12**, 3450 (2023).

[21] R. Kheder, R. Ghayoula, A. Smida, I. El Gmati, L. Latrach, W. Amara, A. Hammami, J. Fattahi, and M. I. Waly, Telecom **5**, 451 (2024).

[22] A. M. Titu, A. V. Sandu, A. B. Pop, Ş. Ţîţu, and T. C. Ciungu, IOP Conference Series: Materials Science and Engineering **374**, 012054 (2018).

[23] G. Hosoi, M. Nitta, S. Saito, H. Suganuma, and F. Maehara, IEICE Communications Express **12**, 96 (2023).